Published in final edited form as:
Biol Bull. 1999 February 1; 196(1): 52–56.

Free Radicals and Chemiluminescence as Products of the Spontaneous Oxidation of Sulfide in Seawater, and Their Biological Implications

DAVID W. TAPLEY[1,*], **GARRY R. BUETTNER**[2], and **J. MALCOLM SHICK**[1]

[1]Department of Zoology and Center for Marine Studies, University of Maine, Orono, Maine 04469-5751

[2]ESR Facility/EMRB 68, College of Medicine, The University of Iowa, Iowa City, Iowa 52242-1101

Abstract

The discovery of symbioses between marine invertebrates and sulfide-oxidizing bacteria at deep-sea hydrothermal vents and in other high-sulfide marine environments has stimulated research into the adaptations of metazoans to potentially toxic concentrations of sulfide. Most of these studies have focused on a particular action of sulfide—its disruption of aerobic metabolism by the inhibition of mitochondrial respiration—and on the adaptations of sulfide-tolerant animals to avoid this toxic effect (1). We propose that sulfidic environments impose another, hitherto overlooked type of toxicity: exposure to free radicals of oxygen, which may be produced during the spontaneous oxidation of sulfide, thus imposing an oxidative stress. Here we present evidence that oxygen- and sulfur-centered free radicals are produced during the oxidation of sulfide in seawater, and we propose a reaction pathway for sulfide oxidation that is consistent with our observations. We also show that chemiluminescence at visible wavelengths occurs during sulfide oxidation, providing a possible mechanism for the unexplained light emission from hydrothermal vents (2, 3).

In the presence of molecular oxygen and trace metal catalysts, hydrogen sulfide spontaneously oxidizes. Oxidation-reduction reactions frequently involve free-radical intermediates, and a metal-catalyzed pathway in which the initial reactions of sulfide oxidation form superoxide and sulfide radicals has been proposed (4). The proposed reaction begins with four steps:

$$HS^- + O_2 \rightarrow HS^\bullet + O_2^{\bullet -} \quad (1)$$

$$HS^\bullet + O_2 \rightarrow HO_2^\bullet + S \quad (2)$$

$$HS^\bullet + O_2^{\bullet -} \rightarrow S + HO_2^- \quad (3)$$

At near-neutral pH, HO_2^- will immediately protonate:

*Present address: Department of Biology, Salem State College, 352 Lafayette St., Salem, MA 01970-5353.

$$HO_2^- + H^+ \rightarrow H_2O_2 \quad (4)$$

The proposed metal-catalyzed mechanism underlying reaction 1 is (4):

$$M^{n+} + O_2 \rightarrow M^{(n+1)+} + O_2^{\bullet -} \quad (5)$$

$$M^{(n+1)+} + HS^- \rightarrow M^{n+} + HS^{\bullet} \quad (6)$$

Notice that, once either radical is formed, a chain reaction ensues. The superoxide that is formed can undergo a subsequent reduction or dismutation to form hydrogen peroxide (H_2O_2), a known product of sulfide oxidation (5, 6), which is also produced in reactions 3 and 4. In the presence of transition-metal catalysts, superoxide and H_2O_2 will react to form the hydroxyl radical, $HO^{\bullet}$, perhaps the most oxidizing radical that can arise in a biological setting.

A similar pathway, in which reaction 2 yields an addition product, was proposed later (7):

$$HS^{\bullet} + O_2 \rightarrow HSO_2^{\bullet} \quad (7)$$

According to this mechanism, the addition product then reacts with molecular oxygen:

$$HSO_2^{\bullet} + O_2 \rightarrow HSO_4^{\bullet} \quad (8)$$

A subsequent series of reactions produces a variety of reactive intermediates, including superoxide, hydrogen peroxide, and the sulfide radical (7).

Although these free-radical mechanisms for sulfide oxidation have been proposed (4, 7), no direct experimental support for such a mechanism has been provided to date. We have therefore employed electron paramagnetic resonance (EPR) spin trapping to gather direct evidence that free-radical intermediates are produced during sulfide oxidation. EPR spectrometry is similar to nuclear magnetic resonance (NMR) spectrometry, but relies on magnetic moments resulting from unpaired electrons instead of those from the atomic nucleus. Samples are exposed to microwave radiation at a fixed wavelength and amplitude while a magnetic field is swept through an appropriate range of field densities. At appropriate combinations of wavelength and magnetic field strength, the unpaired electrons will resonate, thereby absorbing microwave energy. This absorbance is recorded as the first derivative. In an EPR spectrum, the relative positions of peaks (lines) are more important than their absolute positions, so spectra typically are plotted with no abscissa, only a scale bar indicating the change in magnetic field strength over a given distance. The ordinate is in arbitrary absorbance units. Spin trapping is a technique for detecting ephemeral radicals by providing a molecule that preferentially reacts with them, forming more stable radical adducts with characteristic spectra. These spectra typically result from a primary peak, due to the radical that was trapped, being split one or more times by adjacent paramagnetic

nuclei, typically hydrogen and nitrogen. The splitting of peaks is the result of the magnetic moments of the adduct being oriented either parallel or antiparallel to the magnetic moments of adjacent nuclei, with either orientation being equally likely. The magnetic field of half of the population of adducts will be incrementally increased, while that of the other half will be equally decreased. The values of these splittings (a^N and a^H) for various adducts of spin-trapping agents are well known and have been tabulated.

When sulfide was introduced into artificial seawater (ASW) containing the spin-trapping agent dimethylpyrroline-N-oxide (DMPO), a prominent EPR spectrum was obtained (Fig. 1A, B). The greater intensity of the high-field line compared to the low-field line is consistent with ongoing free radical formation by oxidizing sulfide, since the high-field line is detected by the EPR spectrometer several seconds after the low-field line. The appearance of a four-line spectrum with a total width of approximately 45 G suggests that the DMPO-hydroxyl radical adduct (DMPO/$HO^{\bullet}$; $a^N = a^H = 14.9$G) is present (8). But the asymmetry suggests that there are at least two radical species. The second radical should have hyperfine splittings that would produce asymmetries in the two middle lines, yet have a total spectral width near that of DMPO/$HO^{\bullet}$. Appropriate candidates are the sulfide radical adduct, DMPO/$S^{\bullet-}$ ($a^N = 16.09$G, $a^H = 16.19$G) and the sulfite radical adduct, DMPO/$^{\bullet}SO_3^-$ ($a^N = 14.5$G, $a^H = 16.0$G) (8, 9). The splittings for DMPO/$S^{\bullet-}$ are inconsistent with the spectra we obtained; but a computer simulation of the composite of DMPO/$HO^{\bullet}$ and DMPO/$^{\bullet}SO_3^-$ (Fig. 1C) reproduces the experimental spectrum well.

Chen and Morris (4) postulated superoxide production in their reaction mechanism, but the experiment shown in Figure 1 does not directly support this proposal. However, trapping superoxide is difficult, first because the k_{obs} for its reaction with DMPO is low ($\approx 30\ M^{-1} \cdot s^{-1}$ at pH 7.4; *cf*. k_{obs} for DMPO/$HO^{\bullet}$ formation is approximately $3.4 \times 10^9\ M^{-1} \cdot s^{-1}$) (10, 11), and also because the superoxide adduct (DMPO/$^{\bullet}OOH$) can undergo further reactions, including reductions (12), to form DMPO/$HO^{\bullet}$ or EPR-silent products (10, 12). We included DMSO in the reaction mixture to distinguish between these potential routes by which DMPO/$HO^{\bullet}$ can form (Fig. 1D, E). The rate constants for the reactions of $HO^{\bullet}$ with DMPO and DMSO are $3.4 \times 10^9\ M^{-1} \cdot s^{-1}$ and $7 \times 10^9\ M^{-1} \cdot s^{-1}$, respectively (11, 13). Under our reaction conditions DMSO should have scavenged about 96% of the $HO^{\bullet}$ formed; however, the relative abundance of DMPO/$HO^{\bullet}$ in the composite spectrum decreased by only 33%, from 30% to 20% of the composite area (Fig. 1E). This implies that some DMPO/$HO^{\bullet}$ is formed artifactually (10, 14). The DMPO/$HO^{\bullet}$ adduct can also arise from nucleophilic substitution reactions of spin adducts (14 and references therein). For example, DMPO/$^{\bullet}OSO_3^-$ will hydrolyze to DMPO/$HO^{\bullet}$ in aqueous solution. Although formation of $SO_4^{\bullet-}$ is possible in our experiments, no evidence for DMPO/$^{\bullet}OSO_3^-$ ($t_{1/2} = 95$s) was seen in the spectra collected. But our data do not rule out the possibility that hydrolysis gave rise to a portion of the DMPO/$HO^{\bullet}$ observed. The presence of sulfide, a strong reductant, suggests that direct reduction of DMPO/$^{\bullet}OOH$ to DMPO/$HO^{\bullet}$ (12) may have occurred in these experiments.

The conjecture—that superoxide is produced during sulfide oxidation, but is not detected by spin trapping—is supported by investigations into the mechanisms of thiol oxidation. Superoxide can be produced during the oxidation of thiols (15–17), but it is difficult to spin

trap. In most experiments, superoxide production is demonstrated indirectly by including a molecular probe that is indicative of it. We were unable to find a probe for superoxide that would not react with sulfide, and were thus unable by this method to demonstrate superoxide production; but the results when DMSO is included in the reaction mixture, as well as the analogy with thiol oxidation, strongly suggest that superoxide is produced but not detected in our experiments.

The reaction mechanism proposed by Chen and Morris postulates the production of the sulfide radical (reaction 1), but no direct evidence for its formation is yet available. The sulfide radical has been spin trapped in anoxic conditions (9), but in our oxic experiments, conversion of the sulfide radical to oxygenated products appears to be efficient.

Since the reaction pathways discussed above (reactions 1–8) were first proposed, some of the postulated reactions, as well as other reactions relevant to the mechanism, have been demonstrated and their kinetics quantified. We suggest that reaction 2 is not likely to predominate; we propose instead that the addition reaction (reaction 7) predominates (k_6 = $7.5 \times 10^9\ M^{-1} \cdot s^{-1}$ at pH 7) (18, 19) and its product is then immediately deprotonated at near-neutral pH:

$$HSO_2^{\bullet} \leftrightarrow H^+ + SO_2^{\bullet -} \quad (9)$$

Kinetic data for reaction 2 are not available (18), but the rate is not likely to exceed that of reaction 7.

Once $SO_2^{\bullet -}$ is formed, it can oxidize to yield SO_2 and $O_2^{\bullet -}$ ($k_{10} = 1 \times 10^8\ M^{-1} \cdot s^{-1}$ at pH 6.5) (20), which will subsequently hydrate to form HSO_3^-:

$$SO_2^{\bullet} + O_2 \rightarrow SO_2 + O_2^{\bullet -} \quad (10)$$

$$SO_2 + H_2O \rightarrow H^+ + HSO_3^- \quad (11)$$

If a strongly oxidizing radical is present, HSO_3^- will be oxidized to $SO_3^{\bullet -}$. For example, it will react with $HO^{\bullet}$ ($k = 5.1 \times 10^9\ M^{-1} \cdot s^{-1}$ at pH 11.2) (21):

$$HSO_3^- + HO^{\bullet} \rightarrow SO_3^{\bullet -} + H_2O \quad (12)$$

Our results (Fig. 1) strongly suggest the presence of such an oxidizing radical. Therefore, we propose that the reaction sequence 1, 7, and 9–12 occurs during the oxidation of sulfide. This sequence produces both oxygen- and sulfur-centered radicals, and is consistent with the results of our EPR spin-trapping study (Fig. 1). The oxidation of sulfide is catalyzed by trace metals (4) (see below). Therefore we believe that first-chain initiation is accomplished by reaction 6.

Sulfide-generated free radicals could impose an oxidative challenge to tissues exposed to them, and could represent a previously unrecognized type of sulfide toxicity: oxidative stress

resulting from chronic, subacute exposure to sulfide. Marine animals living in environments where sulfide and molecular oxygen coexist are at risk from exogenously formed free radicals, as well as from radicals resulting from sulfide oxidation within their own tissues. This is true in spite of generally hypoxic conditions in sulfidic environments, since the presence of a strong reductant (sulfide) will enhance the production of free radicals (Fig. 1). We have evidence from studies on protobranch bivalves that sulfide exposure does impose an oxidative stress on these animals, and that they possess thermolabile defenses against this (22). Spectra similar to that in Figure 1B are obtained when sulfide is added to heat-denatured homogenates of tissues from the protobranch bivalves *Solemya velum* and *Yoldia limatula*, but are reduced or absent if undenatured homogenates are used (22).

A free-radical mechanism of sulfide toxicity might explain the symptoms associated with subacute sulfide poisoning in humans and laboratory animals. The primary symptom of subacute hydrogen sulfide poisoning is local inflammation of moist tissues exposed to the gas (6, 23, 24), especially the conjunctivae of the eye and the respiratory epithelia. In particular, sulfide-induced pulmonary edema is similar to that which appears under pulmonary oxidative stress (6, 25). Since these symptoms are restricted to moist tissues, the mechanism of irritation probably involves the aqueous reactions of hydrogen sulfide, including those producing radicals.

Evidence for metal catalysis of sulfide oxidation is provided by sulfide-depletion studies (Fig. 2) and chemiluminescence studies (Fig. 3). The rate at which sulfide disappears from solution (Fig. 2) decreases to control levels when the transition metal chelator diethylenetriaminepentaacetic acid (DTPA) is included in the system. This is consistent with previous studies demonstrating catalysis of sulfide oxidation by trace metals (4). The chemiluminescence plots for 200 and 500 μM sulfide (Fig. 3) show little or no induction period. When ethylenediaminetetraacetic acid (EDTA), which leaves one of the d-orbitals of iron available for reaction, is included in the system, a distinct induction period is seen. When DTPA, which coordinates all the d-orbital electrons of ferric iron, is included, light emission is reduced to blank rates. This suggests that trace iron is the primary transition metal catalyst under the conditions of this study (10).

The weak chemiluminescence at visible wavelengths observed during sulfide oxidation (Fig. 3) provides a potential mechanism for light production at the deep-sea hydrothermal vents (2, 3), as suggested by Hastings (in ref. 2). Pelli and Chamberlain (26) have proposed that thermal black-body radiation is a source of visible light. However, since the vent plumes contain millimolar concentrations of sulfide and are mixing with the ambient oxygenated seawater, the conditions necessary for sulfide-dependent chemiluminescence to occur are present. To determine whether chemiluminescence is a source of light at the vents, spectra from the vent plumes must be compared with those from sulfide oxidation. Sulfide oxidation spectra should preferably be determined at the temperature and pressure found at the vents, and the measurement should be made with a low-resolution, high-sensitivity spectrograph of the type under consideration for future vent work (2).

The results presented here have established that both oxygen- and sulfur-centered free radicals are produced during the oxidation of sulfide, and that this is accompanied by

measurable chemiluminescence at visible wavelengths. Production of free radicals during sulfide oxidation has the potential for imposing an oxidative stress on organisms living in sulfidic environments, with ramifications in toxicology, physiology, and clinical medicine.

Acknowledgments

We thank Dr. James North for help with the SIMEPR software. Funding was provided by grants from the Association of Graduate Students and a research assistantship from the Center for Marine Studies at the University of Maine.

Literature Cited

1. Childress JJ, Fisher CR. The biology of hydrothermal vent animals: physiology, biochemistry, and autotrophic symbioses. Oceanogr Mar Biol Annu Rev. 1992; 30:337–441.
2. LITE Workshop Participants. Light in Thermal Environments (LITE). National Science Foundation and National Aeronautics and Space Administration; Woods Hole, MA: 1993.
3. Van Dover CL, Delaney J, Smith M, Cann JR. Light emission at deep-sea hydrothermal vents. EOS. 1988; 69:1498.
4. Chen KY, Morris JC. Oxidation of sulfide by O_2: catalysis and inhibition. J Sanit Eng Div Proc Am Soc Civ Eng. 1972; 98:215–227.
5. Bittersohl G. Beitrag zum toxischen Wirkungsmechanismus von Schwefelwasserstoff. Z Gesamte Hyg Grenz. 1971; 17:305–308.
6. National Research Council. Hydrogen Sulfide. University Park Press; Baltimore: 1979.
7. Kotronarou A, Hoffmann MR. Catalytic autoxidation of hydrogen sulfide in wastewater. Environ Sci Technol. 1991; 25:1153–1160.
8. Buettner GR. Spin trapping: ESR parameters of spin adducts. Free Radical Biol Med. 1987; 3:259–303. [PubMed: 2826304]
9. Bilski P, Chignell CF, Szychlinski J, Borkowski A, Oleksy E, Reszka K. The photo-oxidation of organic and inorganic substrates during UV-photolysis of nitrite anion in aqueous solution. J Am Chem Soc. 1992; 114:549–556.
10. Buettner GR, Mason RP. Spin-trapping methods for detecting superoxide and hydroxyl free radicals *in vitro* and *in vivo*. Methods Enzymol. 1990; 186:127–133. [PubMed: 2172700]
11. Finkelstein E, Rosen GM, Rauckman EJ. Spin trapping. Kinetics of the reaction of superoxide and hydroxyl radicals with nitrones. J Am Chem Soc. 1980; 102:4994–4999.
12. Rosen GM, Freeman BA. Detection of superoxide generated by endothelial cells. Proc Natl Acad Sci USA. 1984; 81:7269–7273. [PubMed: 6095281]
13. Dorfman, LM.; Adams, GE. Reactivity of the Hydroxyl Radical in Aqueous Solutions. U.S. Government Printing Office, U.S. National Bureau of Standards; Washington, DC: 1973.
14. Davies MJ, Gilbert BC, Stell JK, Witwood AC. Nucleophilic substitution reactions of spin adducts. Implications for the correct identification of reactions intermediates by EPR/spin trapping. J Chem Soc Perkin Trans. 1992; 2:333–335.
15. Misra HP. Generation of superoxide free radical during the autoxidation of thiols. J Biol Chem. 1974; 249:2151–2155. [PubMed: 4206550]
16. Saez G, Thornalley PJ, Hill HAO, Hems R, Bannister JV. The production of free radicals during the autoxidation of cysteine and their effect on isolated rat hepatocytes. Biochim Biophys Acta. 1982; 719:24–31. [PubMed: 6293586]
17. Buettner GR, Hall RD. Superoxide, hydrogen peroxide, and singlet oxygen in hematoporphyrin derivative, -cysteine, -NADH and light systems. Biochim Biophys Acta. 1987; 823:501–507. [PubMed: 3030441]
18. Ross, AB.; Mallard, WG.; Helman, WP.; Buxton, GV.; Huie, RE.; Neta, P. NDRL-NIST Solution Kinetics Database: Ver. 2.0. National Institute of Standards and Technology; Gaithersburg, Maryland: 1994.

19. Mills G, Schmidt KH, Matheson MS, Meisel D. Thermal and photochemical reactions of sulfhydryl radicals. Implications for colloid photocorrosion. J Phys Chem. 1987; 91:1590–1596.

20. Creutz C, Sutin N. Kinetics of the reactions of sodium dithionite with dioxygen and hydrogen peroxide. Inorg Chem. 1974; 13:2041–2043.

21. Huie RE, Neta P. Rate constants for some oxidations of S(IV) by radicals in aqueous solution. Atmos Environ. 1987; 21:1743–1747.

22. Tapley, DW. PhD thesis. University of Maine; Orono: 1993. Sulfide-dependent oxidative stress in marine invertebrates, especially thiotrophic symbioses.

23. Yant WP. Hydrogen sulphide in industry. Occurrence, effects, and treatment. Am J Public Health. 1930; 20:598–608.

24. Lopez A, Prior MG, Reiffenstein RJ, Goodwin IR. Peracute toxic effects of inhaled hydrogen sulfide and injected sodium hydrosulfide on the lungs of rats. Fundam Appl Toxicol. 1989; 12:367–373. [PubMed: 2714535]

25. Halliwell, B.; Gutteridge, JMC. Free Radicals in Biology and Medicine. Clarendon Press; Oxford, England: 1989.

26. Pelli DG, Chamberlain SC. The visibility of 350°C black-body radiation by the shrimp *Rimicaris exoculata* and man. Nature. 1989; 337:460–461. [PubMed: 15726721]

27. Cavanaugh, GM. Formulae and Methods VI of the Marine Biological Laboratory Chemical Room. Marine Biological Laboratory; Woods Hole, Massachusetts: 1975.

28. Duling DR. Simulation of multiple isotropic spin-trap EPR spectra. J Magn Reson. 1994; 104:105–110.

29. Cline JD. Spectrophotometric determination of hydrogen sulfide in natural waters. Limnol Oceanogr. 1969; 14:454–458.

30. Gonzalez Flecha B, Llesuy S, Boveris A. Hydroperoxide-initiated chemiluminescence: an assay for oxidative stress in biopsies of heart, liver, and muscle. Free Radical Biol Med. 1991; 10:93–100. [PubMed: 1849867]

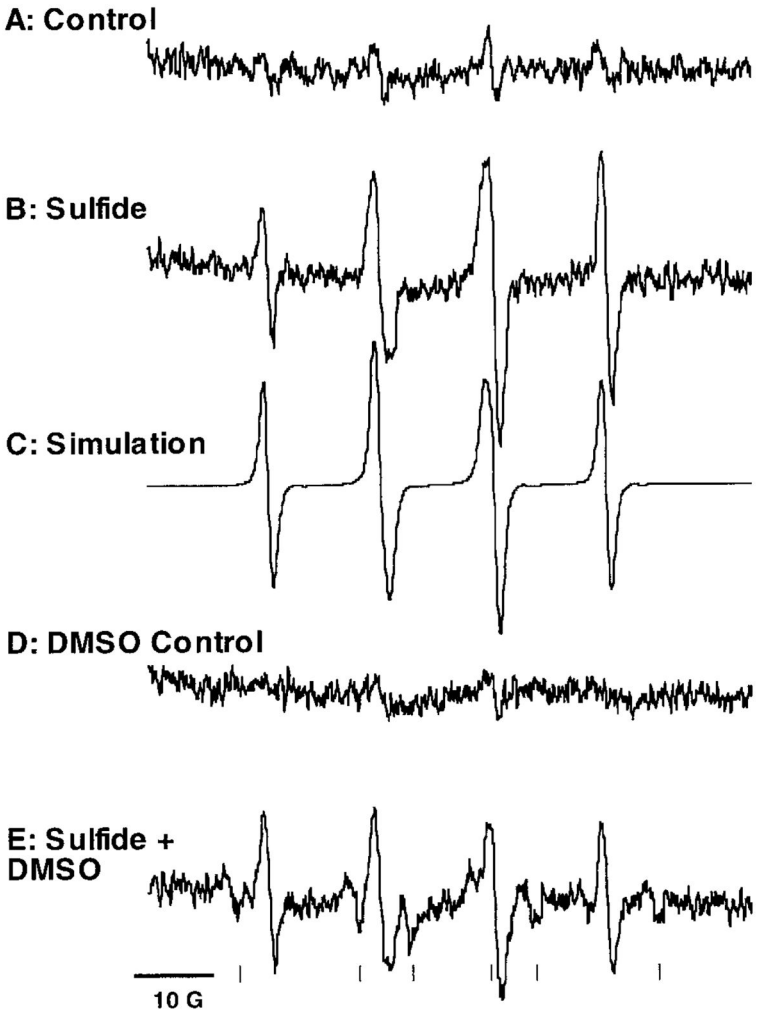

Figure 1.

Electron paramagnetic resonance (EPR) spectra of DMPO adducts formed during sulfide oxidation in air-saturated artificial seawater (ASW) (27) at pH 7.4 and room temperature (≈20°C). (A) Control spectrum of DMPO in ASW with no sulfide added. (B) Spectrum obtained when sulfide (1 m*M*) is added. (C) Computer simulation of the spectrum in B, a composite of DMPO/$HO^{\bullet}$ (30%) and DMPO/$^{\bullet}SO_3^-$ (70%). (D) Control spectrum of DMPO and dimethyl sulfoxide (DMSO) in ASW with no sulfide added. (E) Spectrum obtained when 1 m*M* sulfide is added to DMPO and DMSO in ASW. Computer simulation of this spectrum indicates these relative abundances: DMPO/$HO^{\bullet}$ (20%), DMPO/$^{\bullet}SO_3^-$ (60%), and DMPO/$^{\bullet}CH_3$ (20%). Horizontal scale = 10 gauss; since in this type of spectrometry the relative positions of the lines are more important than their absolute positions, spectra do not usually include an absolute scale. The vertical axis is in arbitrary units. The vertical ticks in (E) mark the positions of DMPO/$^{\bullet}CH_3$ peaks. Reaction components, when present, were in the following final concentrations: DMPO, 50 m*M*; sulfide, 1 m*M*; DMSO, 0.7 *M*. Sulfide was added after all the other reactants, and immediately before transferring the sample to the EPR cell. Spectra were obtained with a Bruker ESP 300 EPR spectrometer equipped with a

TM_{110} cavity and an aqueous flat cell. Computer simulations of spectra were carried out using SIMEPR software (28).

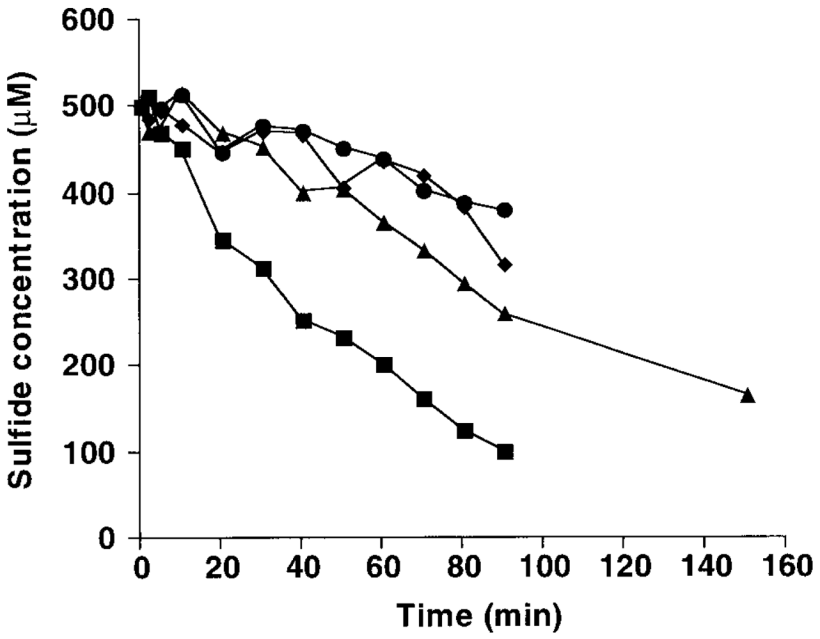

Figure 2.

Time course of the disappearance of sulfide from ASW (pH 7.4) continuously sparged with air or nitrogen gas. Sulfide rapidly disappeared from solution in the aerated treatment (■). When DTPA was present, the loss of sulfide from aerated solution (▲) was reduced to control rates (●: nitrogen-sparged; ◆: nitrogen-sparged, DTPA present). In the anoxic control experiments, as well as those with DTPA, the loss of sulfide was owing to the degassing of H_2S by the nitrogen or air stream, not to the chemical oxidation of sulfide. In experiments where the pH was more acidic (and the proportion of sulfide as H_2S was therefore greater), the loss of sulfide under otherwise identical conditions was greatly increased (data not shown). ASW (50 ml) was placed in a glass Erlenmeyer flask and sparged with air or nitrogen for 1 h before the experiments were begun and continuously thereafter. The experiments were started by addition of sufficient sulfide stock, pH 7.4, to result in an initial sulfide concentration of 500 *μM*. Sulfide concentration was determined at 10-min intervals using the diamine method (29).

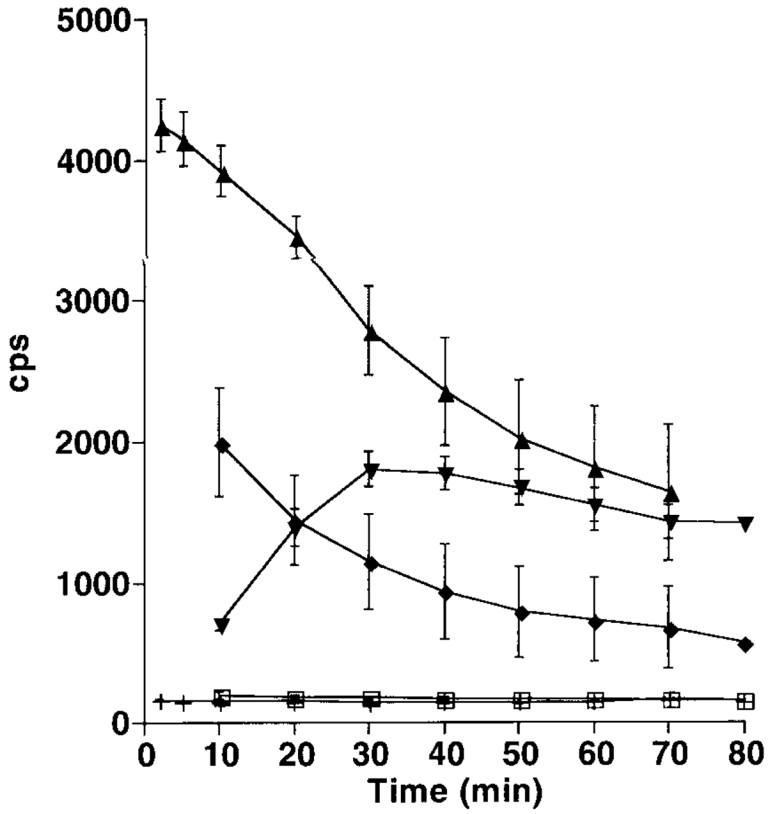

Figure 3.

Time course of chemiluminescence, measured as counts per second (cps), during sulfide oxidation at various initial sulfide concentrations, with and without chelators. Each point is the average of three determinations; error bars are ± one standard deviation. The amount of light emitted was positively correlated with initial sulfide concentration (□: 0 *μM*; ◆: 200 *μM*; ▲: 500 *μM*). Luminescence was reduced substantially, and there was a 30 min induction period, when the chelator EDTA was included in 500 *μM* sulfide (▼). No chemiluminescence was observed in the presence of DTPA and 500 *μM* sulfide (+) or with 500 *μM* sulfide under anoxic conditions (data not shown). Reaction mixtures were prepared in ASW adjusted to pH 7.4 after the addition of chelators, when they were used. Chemiluminescence was measured in a Packard Tri-Carb model 3255 liquid scintillation counter set on the tritium channel in the out-of-coincidence mode (30). The photomultiplier in this counter is sensitive to wavelengths between 380 and 620 nm. Background counts from the empty chamber were 172 ± 4 cps (mean ± SD) and of an empty vial were 186 ± 11 cps. For each determination 20 ml of aerated ASW were placed into a vial, and a sufficient amount of sulfide stock was added to obtain the desired concentration. Counts were accumulated over 10-min intervals; for the experiments employing 500 *μM* sulfide, counts were accumulated over 1-min intervals for the first 10 min.